Plantar pressure distribution of ostrich during locomotion on loose sand and solid ground

Rui Zhang[*], Dianlei Han, Songsong Ma , Gang Luo, Qiaoli Ji, Shuliang Xue, Mingming Yang, Jianqiao Li

Key Laboratory of Bionic Engineering, Ministry of Education, Jilin University, Changchun, P.R. China

Corresponding Author:

Rui Zhang

No. 5988 Renmin Street Nanguan District, Changchun, 130022, P.R. China

Email: zhangrui@jlu.edu.cn

Abstract

Background. Ostrich is a cursorial bird with extraordinary speed and endurance, especially in the desert, and thus is an ideal large-scale animal model for mechanic study of locomotion on granular substrate.

Methods. The plantar pressure distributions of ostriches walking / running on loose sand / solid ground were recorded using a dynamic pressure plate.

Results. The center of pressure (COP) on loose sand mostly originated from the middle of the 3rd toe, which differed from the J-shaped COP trajectory on solid ground. At mid-stance, a high-pressure region was observed in the middle of the 3rd toe on loose sand, but three high-pressure regions were found on solid ground. The gait mode significantly affected the peak pressures of the 3rd and 4th toes ($p = 1.5 \times 10^{-6}$ and 2.39×10^{-8}, respectively), but not that of the claw ($p =$

26   0.041). The effects of substrate were similar to those of the gait mode.

27   **Discussion.** Ground reaction force trials of each functional part showed the 3rd toe bore more
28   body loads and the 4th toe undertook less loads. The pressure distributions suggest balance
29   maintenance on loose sand was provided by the 3rd and 4th toes and the angle between their
30   length axes. On loose sand, the middle of the 3rd toe was the first to touch the sand with a
31   smaller attack angle to maximize the ground reaction force, but on solid ground, the lateral part
32   was the first to touch the ground to minimize the transient loading. At push-off, the ostrich used
33   solidification properties of granular sand under the compression of the 3rd toe to generate
34   sufficient traction.

Introduction

The effective locomotion of terrestrial animals depends on the interaction between the functional body parts and the substrate [1]. Evolution has pushed their environmental adaptation, so the limbs of animals living in different environments show various functional morphology and kinematics. Even the same animal may adopt substrate-specific locomotion strategies. For example, when running on solid surface, the desert-dwelling zebra-tailed lizard (*Callisaurus draconoides*) uses a digitigrade foot posture to recover about 40% of the whole mechanical work [2], but when running on granular surface, the lizard employs a plantigrade foot posture to paddle through granular substrate and generate enough force for acceleration [2, 3].

Despite the complicated interaction between limbs and the ground, recent studies demonstrate both walking and running gaits emerge from a spring-loaded inverted pendulum model, and the gait dynamics vary largely along with different combinations of kinetic energy, leg compliance and leg contact conditions, resulting in different oscillation modes [1, 41, 42]. As for walking, it involves an inverted-pendulum model that accounts for the efficient exchange between potential energy and kinetic energy within each step [4, 5]. Benefiting from this model, humans can not only save 70% of total mechanical work to move body mass at the optimal speed, but also carry up to 20% of body weight on the head without additional energy [4, 6]. Moreover, as for rapid locomotion such as running, hopping and galloping, the center of mass (COM) is inverse to the walking gait, as it minimizes at the mid-stance and maximizes at the touchdown and take-off. Therefore, these bouncing gaits are described as a spring-mass model that accounts for the exchange of mechanical energy. In the spring-mass model, mechanical energy is stored as elastic strain in spring-like tissues (e.g. tendons) at the first half of the stance phase, and then returned by elastic recoil at the second half [4, 5, 7]. Moreover, the spring-mass model could approximate the gait stability of a mammal or bird running on diverse terrains [8, 9]. Although the inverted-pendulum model and the spring-mass model both represent rather simple mechanical systems, these fundamental mechanisms have been observed in humans, birds, cockroaches and lizards, and are utilized to carry out the projects of various bionic robots [9-13].

These models all simplify the substrate as a rigid, flat and perfectly elastic ground, but in reality, natural substrates such as sand, soil and snow display both solid-like and fluid-like features [3]. During movement on natural substrates, solid-fluid transition happens beyond the yield stress and then results in increasing the energy cost and instability of gait [14]. Furthermore, comprehensive models are less well-developed to predict the reaction and leg kinematics on granular substrates than solid substrates. As we all know, soft substrates significantly affect the

70   results.

71   In order to study locomotion on flowing substrates, researchers proved granular dry sand
72   was an ideal substrate, because it displayed both solid-like and fluid-like behaviors and was
73   simpler than other flowing substrates such as snow and soil [15, 16]. Many small and light desert
74   animals, such as lizards, were utilized to study the locomotion mechanics on granular sand
75   because of their high locomotion performance on a wide range of desert terrains [17-19]. It was
76   found natural variation in substrate mechanics did not greatly affect the sprinting performance of
77   either *C. draconoides* or *Uma scorparia*.

78   Moreover, recent studies on the interaction between small legged robots and granular
79   materials (e.g. sand) reveal the effective locomotion on granular materials depends on the
80   solidification properties of the granular substrate [20, 21]. This dependence is partially attributed
81   to the fact that below the yield stress, the forced granular substrate remains solid, but beyond the
82   yield stress, it flows like a fluid. Based on the solidification mechanism, we can explain and
83   predict the rapid legged locomotion on sand by using empirical models [3]. For example, sea
84   turtles, only by using solidification properties of sand under the flippers, can crawl on loose sand
85   at a speed three times the body length per second without any slip [22, 23].

86   Falkingham reconstructed the 3D foot movements of guineafowl traversing a granular
87   substrate from biplanar X-rays, and then incorporated the kinematics into a discrete element
88   simulation [44]. As the soil thickness increased, footprints gradually became shallower and the
89   force acting on sand also decreased. However, these changes can only be qualitatively described.

90   Relevant literatures are focused on small animals, which are convenient for trials. However,
91   plantar pressures in large animals have not been reported. African ostrich (*Struthio camelus*) is
92   an ideal model for locomotion research of large and heavy animals on natural surfaces, as this
93   highly-specialized cursorial bird has extraordinary speed and endurance [24, 25]. This large
94   terrestrial bird moves faster than other ratites and has been filmed running at the speed of 60
95   km·h^{-1} for 30 minutes, with a peak of 80 km·h^{-1} [24, 25]. Ostriches live in deserts, especially
96   semiarid deserts with short grasses, and inhabit about 25 km^2 territories [26]. In order to survive
97   in deserts, ostriches locomote efficiently on diverse substrates (e.g. sand, rocks and grass) to find
98   enough food and water. Compared with bipedal humans, ostriches run at two times speeds with
99   about 50% lower of metabolic cost, although both species have similar weight and height [27,
100   28].

101   This efficient locomotion of ostriches is mechanically supported by the extended jointed

102 chain system of their hindlimbs with the center of mass close to the hip, which maximizes the
103 gravitational and elastic potential energy [25]. Long and slender tendons, coupled with the
104 flexion and extension of joints, store and return a large proportion of mechanical energy, which
105 would otherwise be compensated by muscle power [24, 28, 29]. The permanently elevated
106 metatarsophalangeal joint (MTP) (Fig. 1) is a highly-specialized structure for transforming
107 kinetic energy and gravitational potential energy into elastic strain energy of muscle-tendon units,
108 which accounts for the majority of elastic energy stored in this joint [24, 28]. Furthermore, the
109 longest hindlimb among ratites, in combination with proximally- concentrated muscles, endows
110 ostriches with high stride frequency and large step lengths [29, 30].

111

112
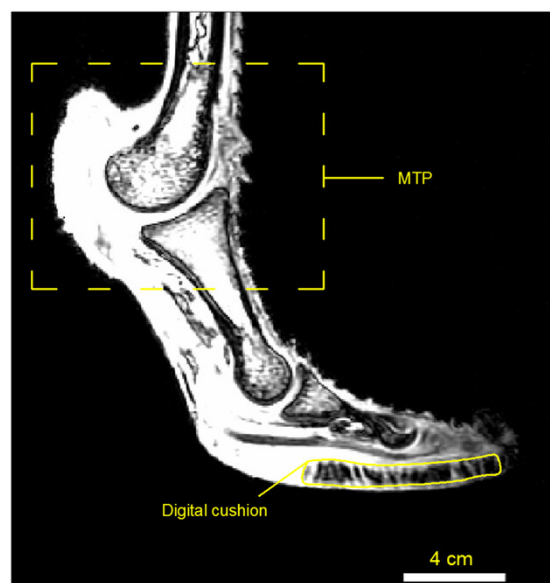
113 **Fig. 1. MRI image of the ostrich foot with the MTP and digit cushion.**

114

115   The adaptation of rapid locomotion can also be observed in ostrich foot toes. Each ostrich
116 foot has only two digits (the 3rd and 4th toes) covered with closely adherent vertical cornified
117 papillae, whereas other ratites have three digits with simple callous plantar pads [30]. The 3rd toe
118 has two approximately parallel digit cushions (Fig. 1) that are fixed by fibrous connective tissues
119 and extend from the 1st to the 4th phalanxes, while the 4th toe has only one cushion under the
120 phalanxes [31]. A recent study on dynamic pressure distribution of ostrich locomotion on solid
121 ground reveals the 3rd toe bears the most loads of the body mass, the 4th toe is responsible for

stabilization and the claw functions as a position anchor [32]. Despite many suggestions about ostrich running rapidly on various terrains, no study has examined the mechanism how the two toes interact with granular materials.

In this study, we explored the plantar pressure distributions of ostrich toes, and assessed the functions of toes when ostriches ran / walked on two typical and well-defined substrates (loose sand and solid ground) that were similar to the habitat environment of ostriches.

Materials and Methods

Animals

Ten healthy juvenile ostriches with healthy feet were selected from a local breeder. Ethical approval was given by the Animal Experimental Ethical Inspection, Jilin University (reference No. 3130089). These ostriches were kept outdoor. Each ostrich was trained to walk and run on a fenced-in corridor for at least 30 minutes each time, twice per day, and over a month before data collection. After comprehensive comparison of representation and amenability, we selected two tractable female adult ostriches to finish all tests. Other female ostrich feet were brought from a slaughter house and then scanned by magnetic resonance imaging (MRI). The three-dimensional reconstruction and MRI images of the feet are shown in Figs. 1 and 2, respectively.

139
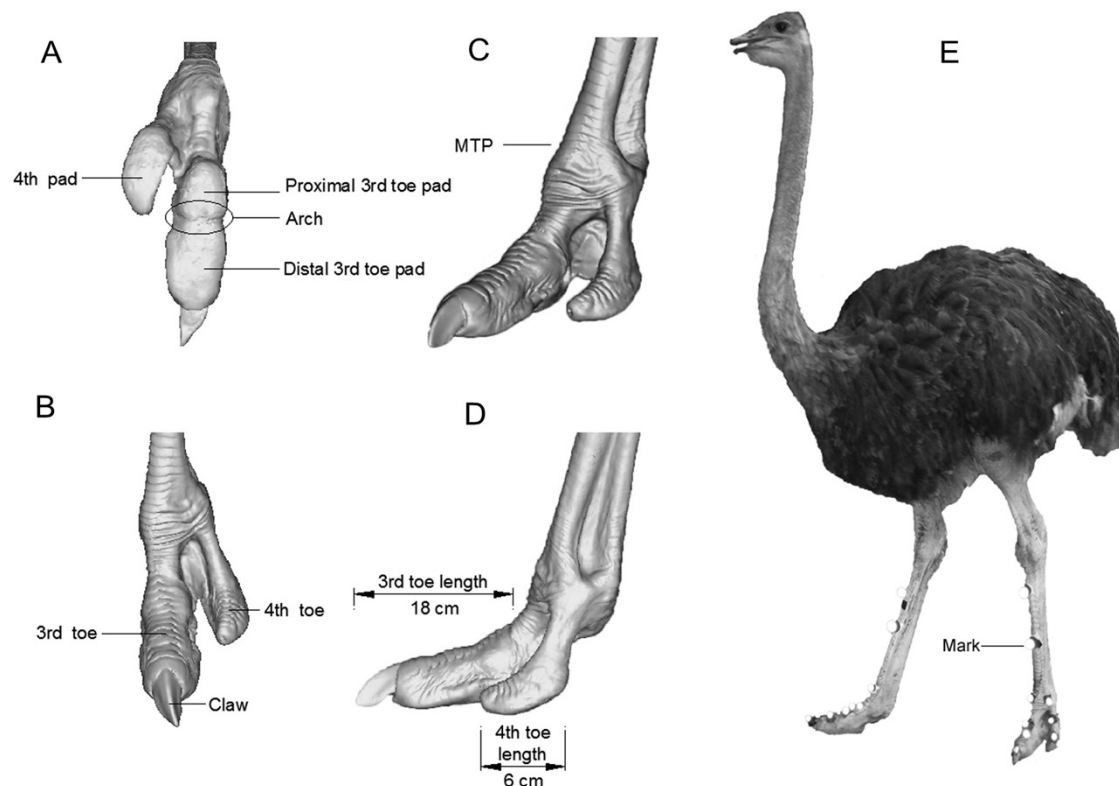
Fig. 2. Three-dimensional reconstruction of ostrich left foot and the model ostrich for trials.
(A) ventral view; (B) front view; (C) isometric view; (D) lateral view; (E) the model ostrich for
trials with marks on its legs.

143

Trackway treatments

An 80-m-long and 2-m-wide runway was constructed near the animal enclosure and fenced
by 1.5-m-tall meshes (Fig. 3). All pebbles or sundries were removed. Within the runway, a
trackway was narrowed to 1.4 m wide and 4 m long where the experimental equipment was
installed. A 6-m-long and 4-m-wide sunshade net was set 3 m above the trackway to prevent any
mistakes induced by sunlight spot in digital reconstruction. In solid ground trials, a custom-
designed polycarbonate frame ($2 \times 1.5 \times 0.015$ m^3) was made to fix the pressure plate. The encased
pressure plate was placed on one level marble slab ($2 \times 1.4 \times 0.03$ m^3) to avoid bending, and
covered with a rubber sheet ($4 \times 1.4 \times 0.0025$ m^3) to avoid potential damage. In loose sand trials,
the trackway was prepared with a 4-cm-thick layer of loose and dry sand to simulate the living
condition in farm and natural desert. The sand thickness was selected with some considerations.

155 If the sand thickness was too large, the effect on plantar pressure would be much more blurry,
156 and the plantar pressure distributions were unclear or even more inaccurate. If the sand thickness
157 was too thin, the action of soft sands on ostrich foot would be ineffective. Therefore, the sand
158 thickness of 4 cm was selected to preliminarily study the plantar pressures of ostriches. The
159 pressure plate and its surrounding components were placed underground, and then the sands
160 were laid on the rubber sheet until the sand surface was leveled with the ground surface. The
161 particle size distribution of sands is shown in Fig. 4. Before each trial on loose sand, the sands
162 were prepared and the level conditions were confirmed to make sure the trackway was in the
163 same state.

164   In each trial, each ostrich ran (or walked) on the loose sand (or solid ground) for at least
165 three valid times, with more details shown in Table 1. The ostrich (1) walked on the solid ground,
166 (2) ran on the solid ground, (3) walked on the loose sand, or (4) ran on the loose sand. Running
167 and walking were classified as the velocity of 2.5-4.1 and 0.7- 1.7 m·s^{-1}, respectively Ground
168 running was not studied in this study.

169

170
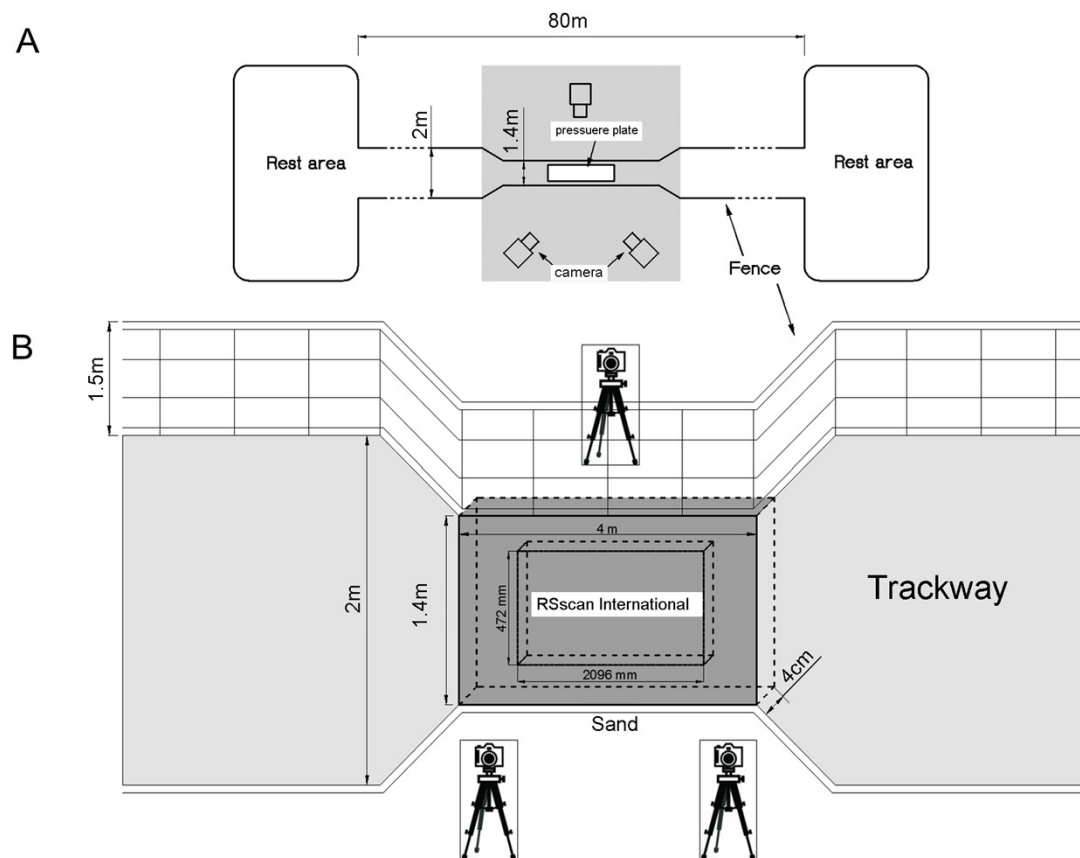
Fig. 3. Schematic of the trackway. (A) Top view; the shade was the data capturing area covered
with the sunshade net. (B) Experimental setup for capture of plantar pressure.

173

174

175
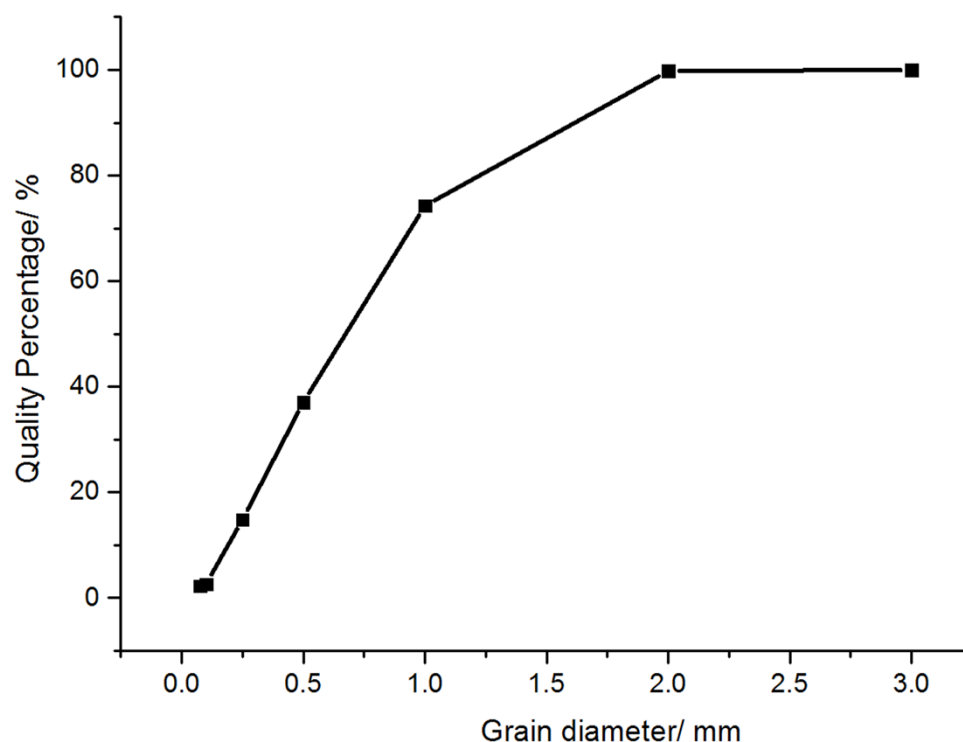
Fig. 4. Particle size distribution of sand used in trackway.

177

Plantar pressure distribution and ground reaction forces

Plantar pressure distribution and ground reaction forces were measured by an RSscan International® pressure plate (2096×472 mm², 500 Hz sampling, 16384 sensors with 0.5 × 0.7 cm², USBII interface; Olen, Belgium). Data were acquired and analyzed on Footscan7 Gait 2nd generation (RSscan International®). Then we divided an ostrich foot into three functional parts: the 3rd toe (without claw), the 4th toe and the claw (Fig. 5) and investigated the effects of each part on locomotion. The ground reaction force of each plantar part was plotted and normalized against body weight. Total ground contact area, the ground contact area of each functional part, and the angle between the 3rd and 4th toes were determined on Footscan7 Gait based on Fig. 5. After the ostrich moved across the sand trackway, we photographed its footprints using an ordinary digital camera. After the surface of the pressure plate was covered with a 4-cm-thick layer of sand, the data of sample weights were inputted into the computer. Then the sample moved on the pressure plate to complete the calibration. The pressure plate was recalibrated after each trial.

192
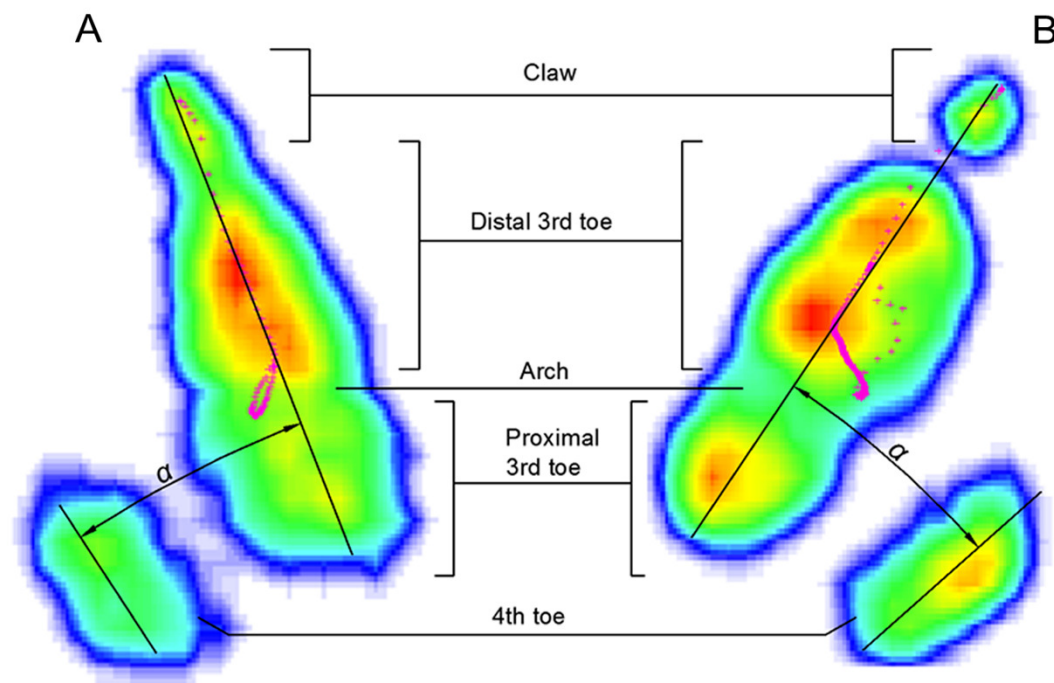
193

194 **Fig.5. Typical Footscan images of plantar surface of the foot in running on loose sand (A)**
195 **and solid ground (B).** Claw, distal 3rd toe, arch, proximal 3rd toe and 4th toe corresponded to
196 different foot parts. α was the angle between 3rd toe and 4th toe.

197

Statistical analysis

198

199   We used analysis of variance (ANOVA) to analyze the differences between two samples,
200 and the effects of gait and media on plantar pressure. Under the condition of walking / running
201 on solid ground / loose sand, we chose indicators of total peak pressure, peak pressure of 3rd toe,
202 peak pressure of 4th toe and peak pressure of claw. Significance level was set at $P < 0.05$. The
203 valid numbers of trials collected and of trials analyzed are shown in Table 1.

204

Table 1. Tests of two samples under different media and gait modes

	Solid ground		Loose sand	
	Walking	Running	Walking	Running
Number of trials collected	10	17	6	11
Number of trials analyzed	10	10	6	6

205

206

207

Results

Center of plantar pressure

209   When the ostrich ran on the loose sand, the COP mostly originated from the middle of the
210 3rd toe (Fig. 6A). The 3rd toe was the first part to touch the loose sand (16 ms), followed
211 immediately by the 4th toe (63 ms) (Fig. 7A), so the COP trajectory moved towards the 4th toe.
212 However, the key function of the 3rd toe was to bear the body weight, and an elliptical COP
213 trajectory appeared in some trials at about the first half of the stance phase. The origin of COP
214 indicates the middle of 3rd toe was the first to touch the sand, followed immediately by the 4th
215 toe. At the last half of the stance phase, COP moved from the middle of the 3rd toe directly to the
216 claw, but the 4th toe gradually left the loose sand (158, 221 and 285 ms; Fig. 7A).

217   Different from the COP trajectory observed in the loose sand trials (Fig. 6A), a J-shaped
218 COP trajectory was found in the solid-ground running trials (Fig. 6B). The areas of ground
219 touching show the 3rd and 4th toes touched the ground simultaneously (16 and 63 ms; Fig. 7B).
220 Therefore, when an ostrich ran on the solid ground, the COP originated from the lateral part of
221 the 3rd toe. During solid-ground running trials, COP followed a similar curve path that it moved
222 from the lateral part to the longitudinal center of the distal 3rd toe, and then straightly to the claw
223 after about 70% of the stance phase (Fig. 6B).

224   In most running trials, the course of COP traversed a longer distance and was closer to the
225 arch on loose sand than on solid ground, which was because the arch contacted with the sand and

226   carried a part of the load (Fig. 6A).

227
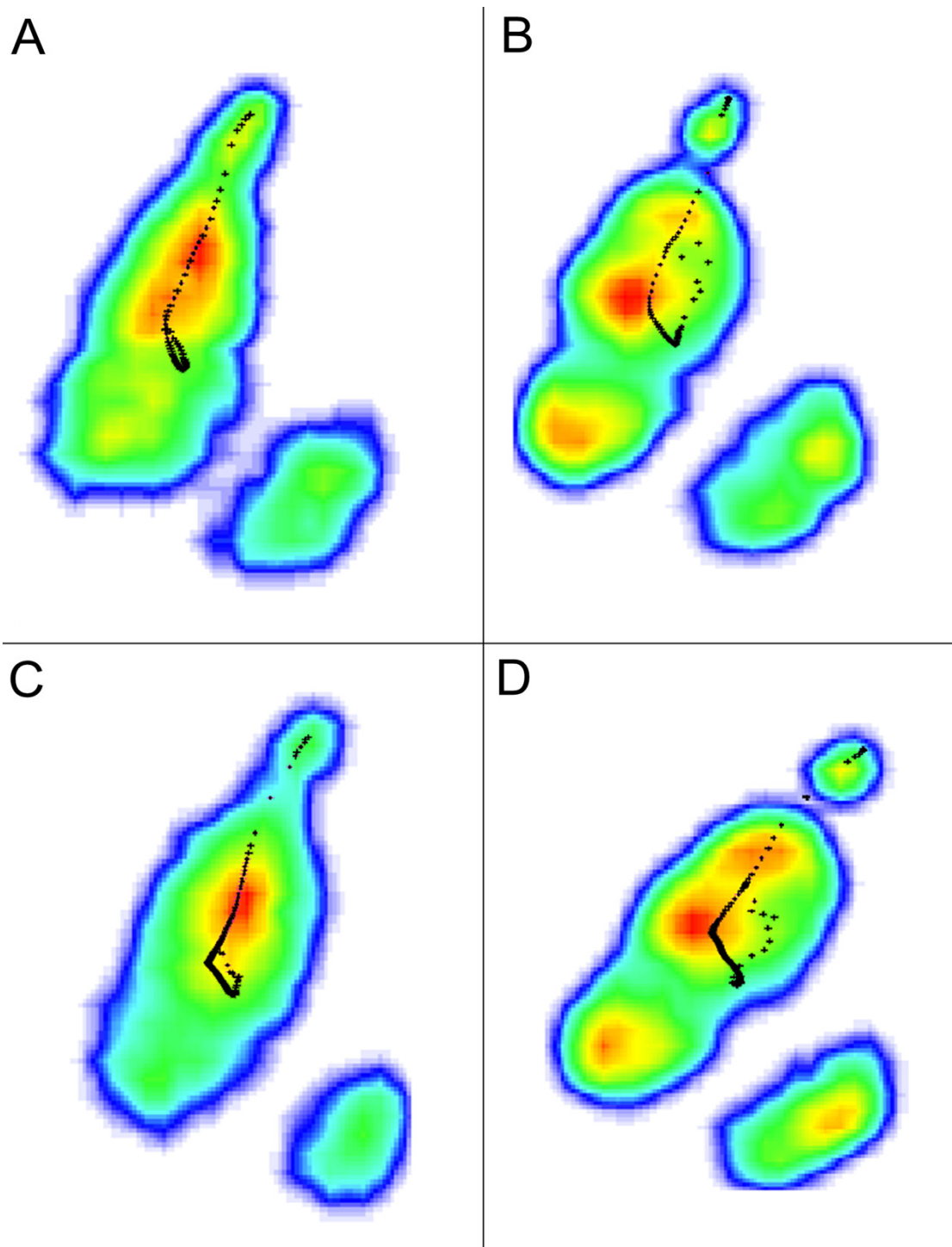
228

229   **Fig. 6. Typical COP path (**shown as black dots**) of the ostrich right foot.** (A) running on loose

230 sand, (B) running on solid ground, (C) walking on loose sand, (D) walking on solid ground. Red,
231 yellow, green and blue indicate the plantar pressure decreased gradually.

232

233   When the ostrich walked on loose sand or solid ground, the COP path originated from the
234 similar position as that in the running trails. On the loose sand, the COP path was more
235 changeable than the one on the solid ground (Fig. 6C). On solid ground, the distal 3rd toe and the
236 4th toe touched down almost simultaneously at the beginning of the stance phase (43 ms, Fig.
237 8B), which provided a stable landing and resulted in a high variable COP distribution at the
238 initial 5% of the stance phase (Fig. 6D).

239

Plantar pressure distribution and roll-off pattern

241   Among all contact elements in the sand running trials, the 3rd toe was the first to touch
242 down, followed by the 4th toe and the claw (Fig. 7A). During ground running trials, the 3rd toe
243 was the first to touch the ground firs, followed by the claw almost immediately and finally the
244 4th toe (Fig. 7B). The sand walking trials involved the same roll-pattern as the sand running
245 trials (Fig. 8A). During ground walking trials, the distal 3rd toe touched down at the beginning of
246 stance phase, followed by the proximal 3rd toe and then the 4th toe (Fig. 8B).

247

248
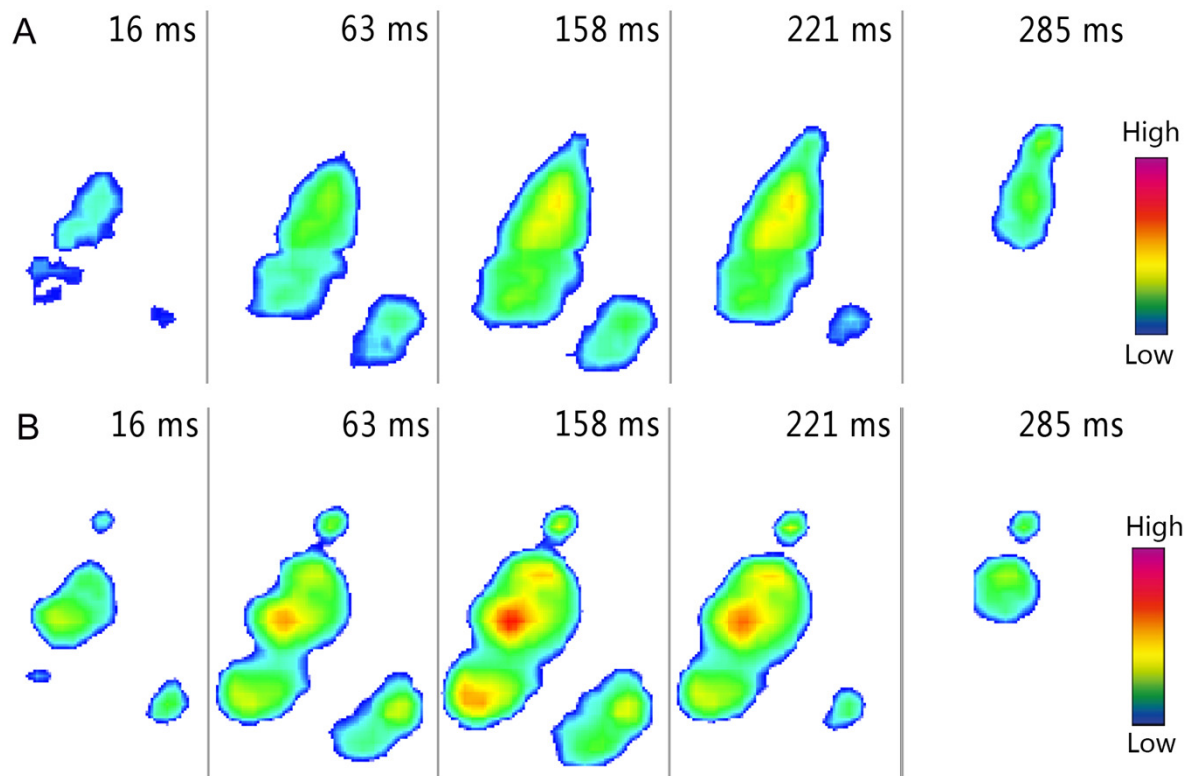
Fig. 7. Roll-off patterns of the right toe during loose sand (A) and solid ground (B) running trials. The images were recorded at 16, 63, 158, 221, and 285 ms after touch-down of foot. Loads were indicated on a gradient from red to dark blue (the same below).

252

253
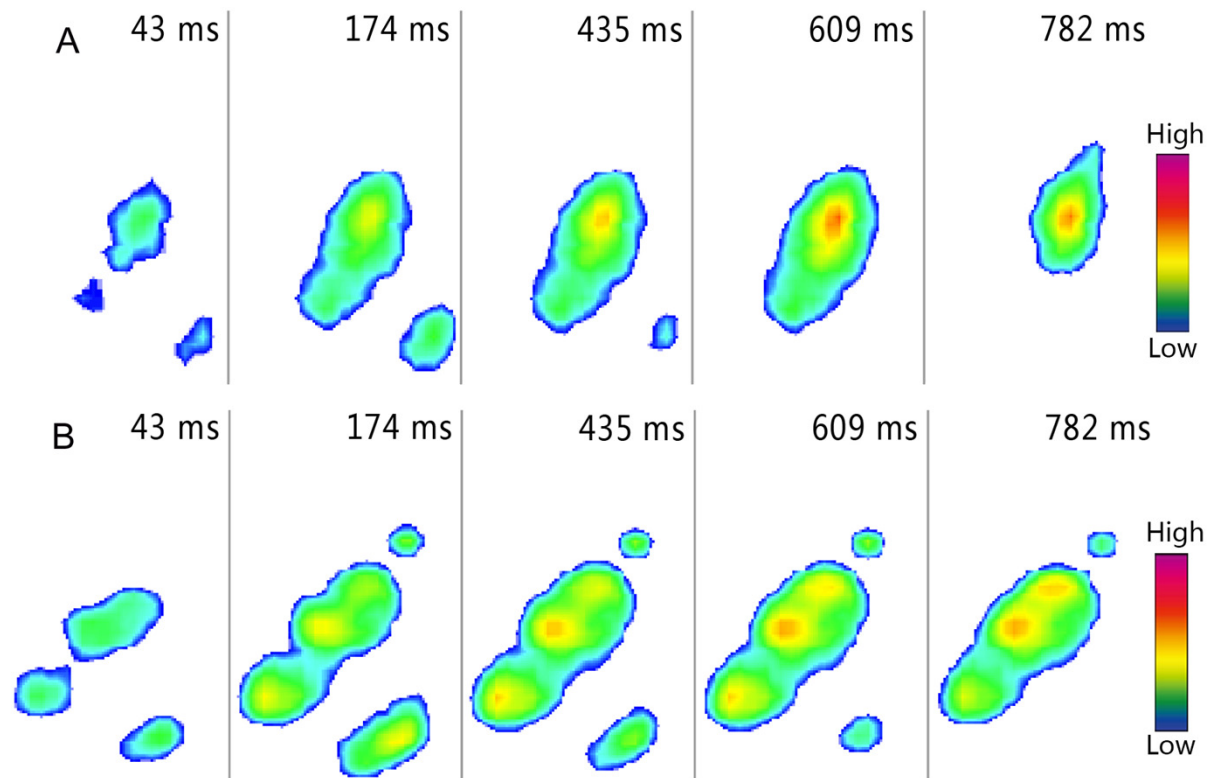
Fig.8. Roll-patterns of right toe during loose sand (A) and solid ground (B) walking trials.
The images were recorded at 43, 174, 435, 609 and 782 ms after touch-down of foot.

256

During sand running trials, a high-pressure region in the middle 3rd toe was observed around the initial contact region at the mid-stance, suggesting the distal 3rd toe bore the most load (Fig. 7A). At toe-off, the sands under the claw carried partial load, which resulted in connecting images between the claw and the distal 3rd toe. Except for a smaller pressure, the plantar pressure distribution of loose-sand walking (Fig. 8A) is the same as that in the running trials. The footprint examination in Fig. 9 supported the pressure distributions. The sand was solidified and flatted under the high-pressure region of the 3rd toe. Furthermore, two distinct sand bulges appeared on the sand surface under the compression of the arch and the claw.

265

266
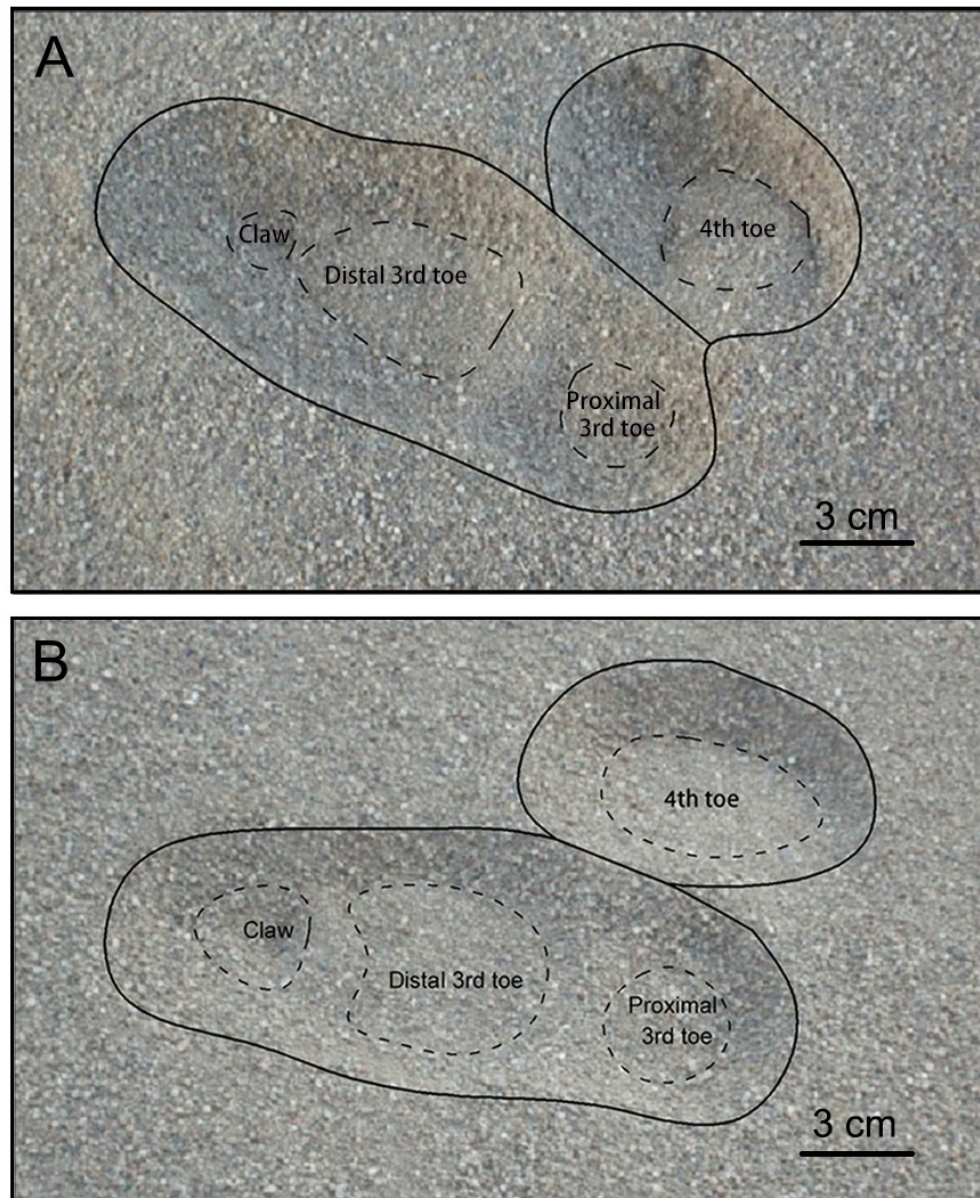
Fig. 9. Footprints of ostrich right foot when (A) running and (B) walking on loose sand. The
black solid lines show the region of disturbed sands. The dashed lines show the region of sand
solidified and flatted by different parts of ostrich foot. An obvious hump appeared between the
distal and proximal parts of the 3rd toe in both running and walking trials.

271

When the ostrich ran on solid ground, almost all parts of toes contacted the ground at the
same time. As showed in Fig. 7B, three high-pressure areas on the 3rd toe and close to the digital

274   joints were found after 20% of the stance phase. During walking trails, the dynamic pressure
275   distribution was consistent with that in running trials except for the lower pressure and the
276   exclusion of the claw from the initial contact period (Fig. 8B). Unlike on loose sand surface, the
277   arch of ostrich foot could be easily identified from the plantar pressure profiles when the ostrich
278   moved on the solid ground.

279   The surface areas on loose sand recorded by the pressure plate are shown in Table 2.
280   Clearly, the total pressure area and the pressure areas of main supported parts of ostrich toes are
281   slightly larger during running trails than walking trails. However, the areas of the claw were
282   about 52.7% larger and the angle αwas 44.1% larger in running trials than in walking trials.
283   When the trials were changed from ground walking to ground running, the load-bearing areas
284   excluded the claw and α increased. The total surface area increased by 11.5% in running trails,
285   which resulted from the 4.4% increase in the area of the 3rd toe and the 36% increase in the area
286   of the 4th toe. In the loose sand trials, however, the area of the claw almost remained
287   unchangeable when the bait was changed from walking to running. Total areas of toes on these
288   two substrates suggest no obvious slip occurred, which was also supported by the qualitative
289   analysis of videos and footprints.

290

Table 2. Plantar surface areas of total foot and functional parts

	Total foot (cm²)	3rd toe (cm²)	4th toe (cm²)	Claw (cm²)	α (°)
Running on loose sand	144.9±7.6	89.9±4.8	41.5±4.2	11.3±3.5	24.5±6.7
Walking on loose sand	133.5±11.1	89.6±5.5	34.9±8.4	7.4±2.7	17.0±9.0
Running on solid ground	159.8±4.5	99.3±3.9	48.4±3.1	11.6±1.7	20.3±3.1
Walking on solid ground	143.3±6.5	95.1±4.5	35.6±5.1	11.1±1.4	19.6±4.9

291   Note:

292   Data are expressed as mean ± standard deviation (the same below).

293

Ground reaction force in running trials

295   The curves of total vertical ground reaction force were similar between different running
296   trials, with a sharp increase at the first half of the stance phase and a quick decrease at the second
297   half (Fig. 10A). The magnitudes of total ground reaction force on loose sand and solid ground
298   were over 2.5 and 1.8 times of body weight, respectively. Among all contact elements during
299   loose sand trials, the 3rd toe attained the maximum load at 50% of the stance phase (Fig. 10B),
300   while the 4th toe reached the peak force at 35% of the stance phase and left the substrate at 69%
301   of the stance phase (Fig. 10C). The forces of the claw were detected at 8% of the stance phase,
302   increased to the peak at 80%, and lasted to the end (Fig. 10D).

303

Sand-running

Body weight

Solid-running

A

B

C

D

Stance phase

304
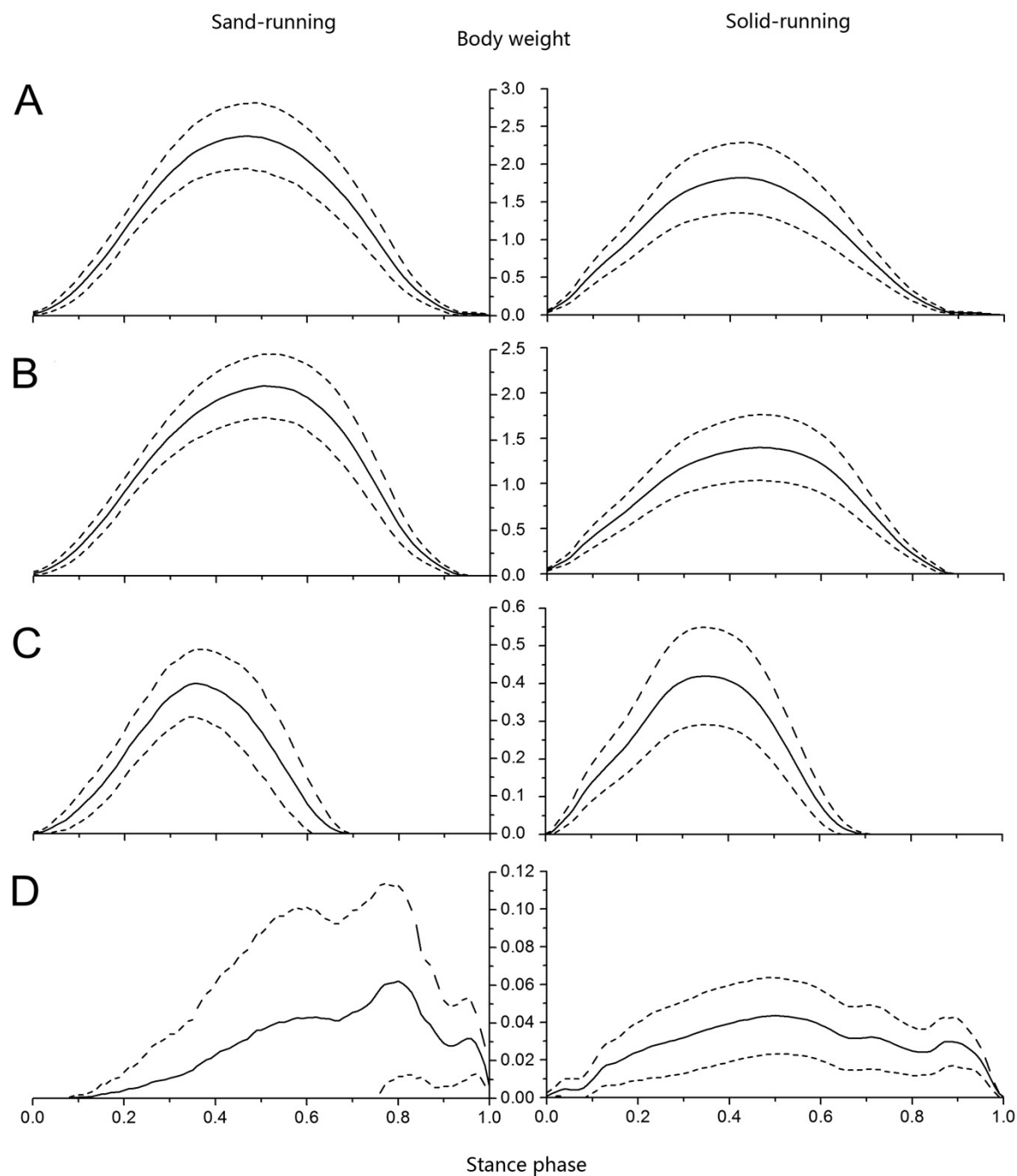
Fig.10. Vertical ground reaction forces versus stance phase during loose sand and solid ground running trials. Vertical ground reaction forces of (A) total foot, (B) 3rd toe, (C) 4th toe, and (D) the claw were all normalized against the body weight. The solid lines and dotted lines stand for the mean and standard deviations, respectively (the same below).

309

310   The loads of contact elements increased simultaneously during solid ground running trials.
311 Firstly, the maximum load on the 4th toe was 34%, and then it shifted to the 3rd toe which
312 attained the vertical peak force at 46% of the stance phase (Fig. 10). Generally, the 3rd toe bore
313 the majority of load, with about 84% and 77% of the entire load during sand and ground trials,
314 respectively, while the 4th toe carried only about 14% and 23% of the entire load during sand
315 and ground trials, respectively. Although the curves of ground reaction forces of total foot, 4th
316 and 3rd toes were all similar between substrates, the curve of the claw was obviously different,
317 as the standard deviations under the claw were larger on sand surface than on solid surface. At
318 toe-off, the vertical peak force shared by the claw was 1.5% and 2.4% of the entire load on loose
319 sand and solid ground, respectively.

Ground reaction force in walking trials

320

321   The profiles of total vertical ground reaction forces in walking trials were slightly different
322 from those recorded in running trails. The profiles in walking trials could be roughly divided into
323 three parts: (1) a quick rise at 20% of the stance phase, (2) a slight increase at 50% of the stance
324 phase, and (3) a rapid drop after about 70% of the stance phase (Fig. 11). The maximum total
325 ground reaction forces on loose sand and solid ground were 1.3 and 1.1 times of the body weight,
326 respectively, which occurred at 73% and 63% of the stance phase, respectively (Fig. 11A). In
327 walking trials, the 4th toe, the 3rd toe and the claw successively attained the peak vertical ground
328 reaction force. During the sand and ground walking trials, the vertical peak forces under the 4th
329 toe were 10.7% and 22.8% of the vertical total forces respectively, and the contact durations
330 between the 4th toe and the substrate were at 76% and 94% of the stance phase, respectively (Fig.
331 11C).

332

333
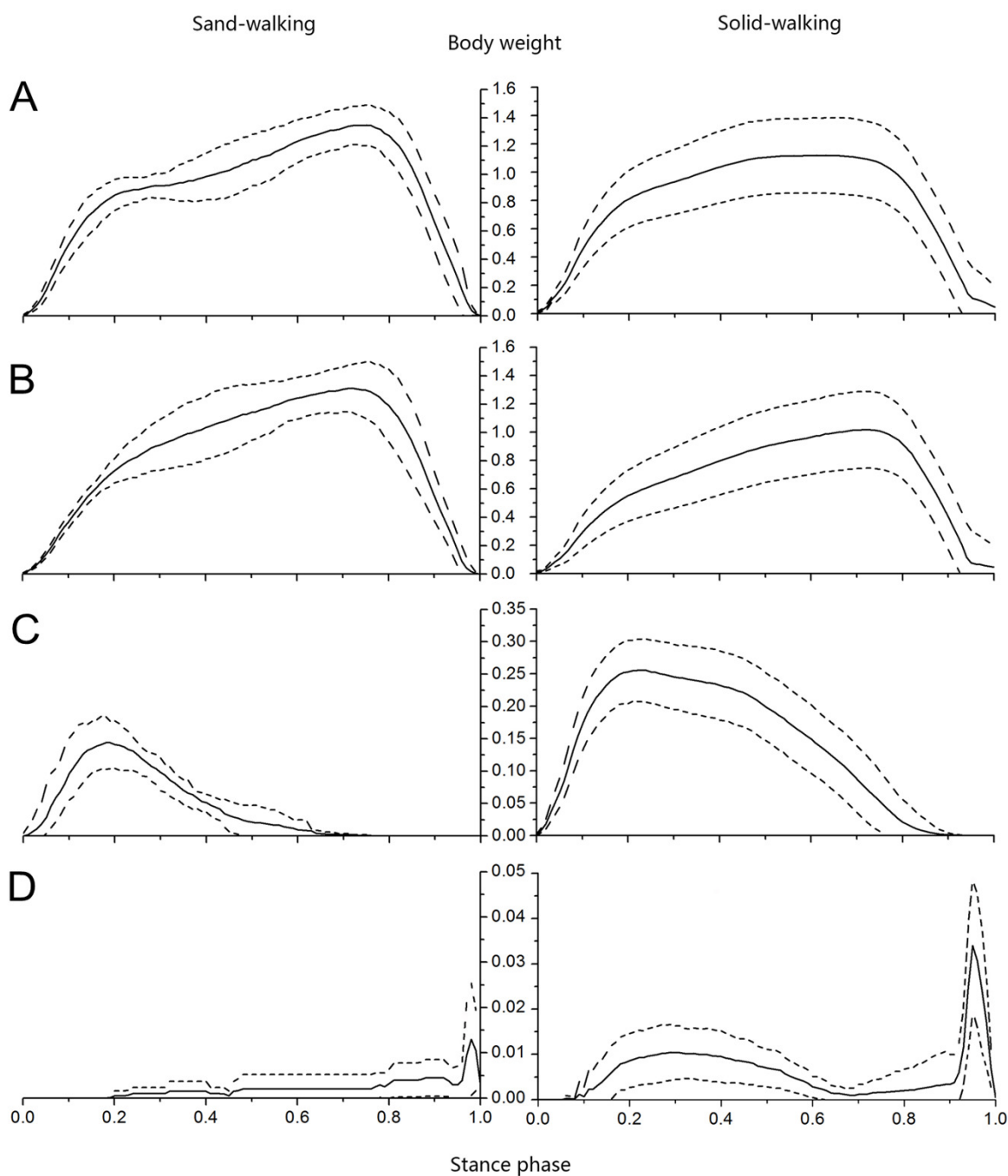
Fig. 11. Vertical ground reaction forces versus stance phase in loose sand and solid ground walking trials. Vertical ground reaction forces of (A) total foot, (B) 3rd toe, (C) 4th toe, and (D) the claw were all normalized against body weight.

337

338 # Results of statistical analysis

339   To analyze whether differences existed between two samples, we selected the peak
340 pressures of different functional parts as indices. The differences in different media and different
341 gaits between two samples were tested via one-way ANOVA. As shown in Table 3, no
342 significant difference was found between the two samples (all p >0.05), so the data of two
343 samples were combined to analyze the significance of the gaits and the media.

344

Table 3. Peak plantar pressures of two samples in different media and gaits

	Sample	Solid ground		Loose sand	
		Walking	Running	Walking	Running
Total	1	1.13 ± 0.290	2.14 ± 0.540	1.49 ± 0.200	2.55 ± 0.560
	2	1.12 ± 0.270	1.87 ± 0.390	1.34 ± 0.160	3.01 ± 0.810
3rd toe	1	1.05 ± 0.300	1.64 ± 0.400	1.48 ± 0.110	2.17 ± 0.510
	2	0.99 ± 0.270	1.39 ± 0.320	1.34 ± 0.160	2.34 ± 0.090
4th toe	1	0.24 ± 0.030	0.48 ± 0.150	0.15 ± 0.025	0.4 ± 0.130
	2	0.28 ± 0.055	0.47 ± 0.095	0.15 ± 0.053	0.4 ± 0.060
Claw	1	0.041 ± 0.006	0.047 ± 0.030	0.014 ± 0.003	0.02 ± 0.010
	2	0.032 ± 0.018	0.047 ± 0.020	0.016 ± 0.016	0.04 ± 0.020

345   Note:

346   No significant inter-individual effects were found at $p < 0.05$.

347   The values were all normalized against the body weight.

348

349   Two factors were analyzed: gait mode (walking vs. running) and media (solid ground vs.
350 loose sand). The data were analyzed using repeated-measures two-way ANOVA. The main

351 effects of gait mode and media were analyzed for each part (total, 3rd toe, 4th toe and claw), and
352 illustrated in terms of F value and p value (Table 4).

353

Table 4. F value and p value with consideration of interaction

	Media		Gait mode		Interaction	
	F value	P value	F value	P value	F value	P value
Total	11.87	0.0018	52.7	6.65×10^{-8}	2.49	0.12
3rd toe	25.49	2.42×10^{-5}	36.89	1.5×10^{-6}	2.47	0.12
4th toe	8.78	0.0061	58.71	2.39×10^{-8}	0.42	0.51
Claw	7.84	0.0091	4.57	0.041	0.27	0.6

354

355 As showed in Table 4, media and gait mode are significant independent factors, but their
356 interaction is not significant. Thus, it can be stated the main effects of both media and gait modes
357 are significant, but the effect on the outcome of the change in gait mode does not depend on the
358 media. To further detect their interaction, we drew interaction plots (Fig. 12).

359

360
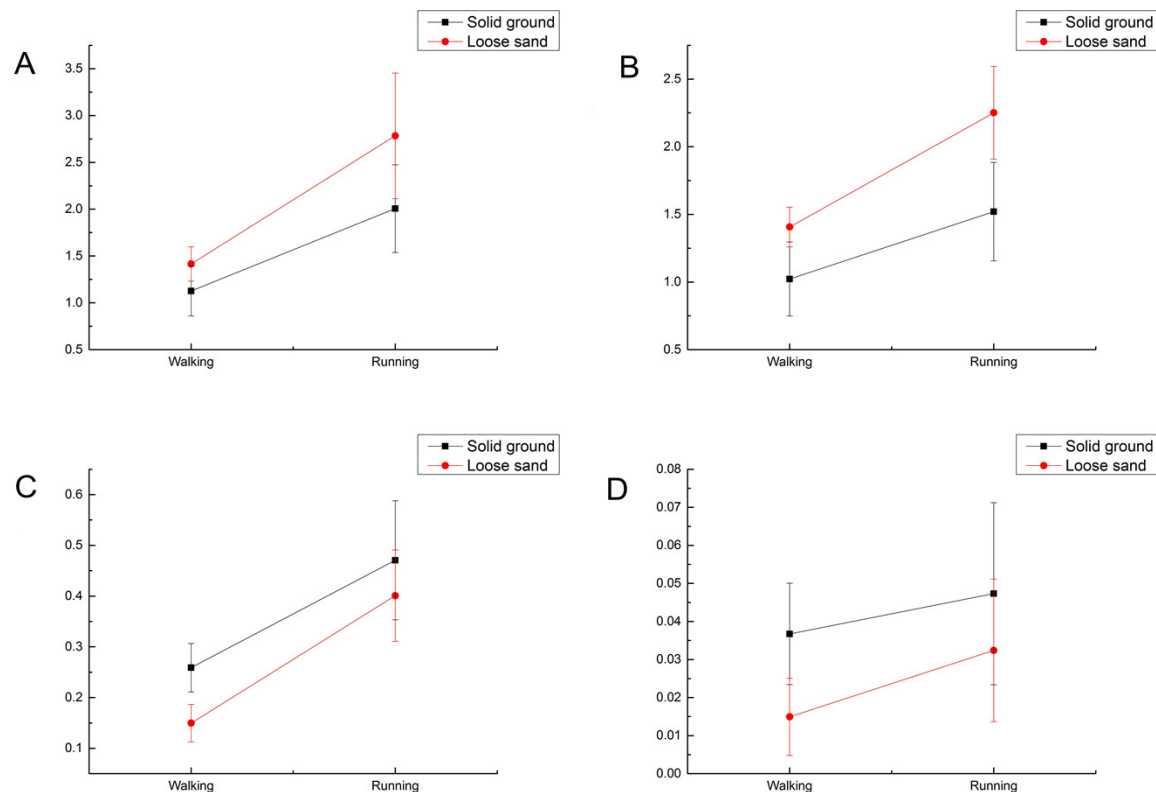
Fig. 12. Peak plantar pressures under different media and gaits. (A)Total force, (B)3rd toe, (C)4th toe, (D)Claw. The values were all normalized against the body weight.

363

364

365   The population means of media and gaits were all significantly different (p <0.05). However, the data in Fig. 12 suggest only a weak interaction between media and gait mode, so we recalculated the effects of the two factors without interaction.

368

Table 5. F value and p value without consideration of interaction

	Media		Gait mode	
	F value	**P value**	**F value**	**P value**

Total	11.29	0.0021	47.81	1.34×10^{-7}
3rd toe	24.25	3.12×10^{-5}	32.75	3.41×10^{-6}
4th toe	8.96	0.0055	61.2	1.25×10^{-8}
Claw	8.04	0.0082	4.4	0.044

369

370 The population means of media and gait mode were still significantly different without
371 consideration of interaction (p<0.05; Table 5).

372

Discussion

373

374 The dynamic pressure distribution and the COP path during solid ground running or walking
375 trials are consistent with a previous study [32]. This consistency in the profiles of ground
376 reaction forces suggests the 3rd toe supports most loads and the 4th helps to maintain body
377 balance. However, there are some differences in the COP path and the magnitude of ground
378 reaction forces between the two studies, which should result from the differences in the collected
379 velocities. Furthermore, our study is unique that we identified three high- pressure regions under
380 the digital joints of the 3rd toe, which suggest the relation between the ground reaction force and
381 the plantar skeleton, as well as the importance of digital cushion in protecting the plantar
382 skeleton and soft tissues.

Locomotion on loose sand

383

384 During loose-sand running, the touchdown of the 3rd toe resulted in a larger heel contact
385 area and a smaller attack angle, compared with solid ground locomotion. The attack angle is
386 between the cross-sectional plane of the 3rd toe and the sand surface. As reported, the vertical
387 reaction force of intruding into granular materials (F_z) can be computed as follows [3]:

388
$$F_z = \delta \times A \times Z$$

389 where δ is the vertical stresses per unit depth, A is the projected intruder surface area, and Z is the
390 intrusive depth. For a given granular material, δ depends on the orientation and moving direction
391 of the intruder. Although the relationship between δ and the intruder behavior is complicated, it

392   is clear a smaller attack angle would increase the reaction force [3]. Thus, the ostrich toe
393   orientation with a smaller attack angle during touchdown on loose sand could generate a stronger
394   reaction force to support its body load. The phalanxes of the 3rd toe left the ground in order,
395   which resulted in a smaller Z. An additional force, which was derived from the arch of the 3rd
396   toe, not only enlarged the contact surface but also solidified the sands under the 3rd toe.

397   During push-off, the 3rd toe did not slip on sand, but the claw continued to intrude into sand.
398   This phenomenon differed from the foot kinematics of zebra-tailed lizard moving on sand, in
399   which the feet paddled through granular materials, generating force with huge energy loss [2,43].
400   The no-slip movement of ostrich toes and claw could be explained by the mechanism of granular
401   material solidification. This mechanism was revealed by the locomotion of sea turtles on
402   granular surfaces, in which the sea turtles created a hard sand region behind its flippers that
403   remained no-slip locomotion [22]. Hence, we estimated the reaction force for advancing
404   locomotion was partly supplied by the solid properties of sands under the toes. Furthermore, our
405   experiments indicate the maximum friction coefficient of a plate could reach 0.65 before slipping
406   during moving on granular medium [33]. Therefore, the combination of the no-slip toes and the
407   dense papillae covered on plantar surface may lead to acceleration because of considerable
408   friction.

409   Our investigation suggests the 4th toe could correct the possible imbalance of the center of
410   body weight on solid ground. Compared to the 3rd toe, the 4th toe shares less loads during the
411   locomotion (particularly walking) on loose sand, which might result from the compensation of
412   balance provided by the 3rd toe with its elliptical morphology. When the 3rd toe is intruding into
413   loose sand, the lateral part could utilize the reaction of sand particles by compressing the sands to
414   reduce the load of the 4th toe [16].

Locomotion on solid ground

416   Repeated transient loading of foot strike, which occurred when the foot touched the ground
417   and then transmitted upward the skeleton and soft tissues, might cause fatigue damage and
418   accelerate running injuries [34, 35]. However, to eliminate the disadvantage of foot strike, the
419   ostrich utilized a special strategy in long-distance running, which had been revealed by human
420   kinematics examination. Abundant evidences show the habitually barefoot endurance runners as
421   well as the running endurance *Homo erectus* landed on ground with the lateral foreparts of their
422   feet, so as to avoid the transient forces [36, 37]. These discrete points of the initial COP, located
423   on the lateral distal part of the 3rd toe, indicate the ostrich landed on the ground with the lateral

424 foreparts of the 3rd toe. During the impact process, the metatarsophalangeal joint flexed and the
425 phalangeal joints extended as the toe moved under the control of tendons and muscles [28].

426   By flexing and extending these joints, ostrich toes partly translated the translational kinetic
427 energy into the rotational kinetic energy of joints, which reduced the effective mass involved in
428 the initial foot-ground contact phase and further decreased the magnitude of the impact transient
429 force [36, 38].

430   It has been suggested a part of foot strike is absorbed by the viscoelastic material located in
431 the interface between the digital phalanx and the ground, especially the adipose cushion [39].
432 The viscoelastic material in ostrich footpad includes the adipose cushion, which consists of
433 numerous adipocytes, a few other connective tissues, and abundant parallel collagen fibers [31].
434 Shock absorption of the viscoelastic material in ostrich footpad was brought by the deformation
435 of fat cells and collagen fibers against the compression. Further studies on the mechanical
436 property of the adipose cushion pad may help to comprehensively understand how the ostrich
437 footpads save energy and reduce the magnitude of transient force [40].

438

439

Perspectives

440

441   Slight errors existed between the plantar pressure and the measured value in the loose sand,
442 which were mainly due to the rolling and sliding of sand particles, and the extrusion and
443 collision between sand particles. However, there is no proper test technology for measurement of
444 large animal plantar pressures, when the large animal running or walking on loose sands. We laid
445 4-cm-thick sand on the pressure plate and tested the plantar pressure could be tested when an
446 ostrich walked or ran on loose sand. Despite some errors in the quantitative measurement of
447 ostrich plantar pressure, this method could be used to analyze the changing rules of ostrich
448 plantar pressure and its proportion in different plantar parts when the ostrich was travelling on
449 sand. Compared with the change rules of ostrich plantar pressure on solid ground, the high
450 efficiency mechanism of ostrich foot travelling on sand could be studied. In the future, we will
451 continue to study the effects of sand thickness on ostrich plantar pressure during sand travelling,
452 and explore the method to accurately measure ostrich plantar pressure in sandy environment.

453

Conclusions

454

455   The COP trajectory originated from the center of the 3rd toe when the ostrich ran on loose
456   sand, which was different from the J-shape COP trajectory found on solid ground. The COP
457   trajectory combined with the pressure distribution of each functional part and the motion of toes,
458   indicating ostrich toes did not play the same functions on different substrates. On loose sand, the
459   enlarged 3rd toe carried more body loads and provided sufficient traction by using the sand-
460   solidification characteristics. The special arch and the well-developed claw of the 3rd toe also
461   played a crucial role during locomotion on loose sand. On solid ground, the lateral part of the 3rd
462   toe touched the ground in the beginning of stance phase, which prevented the skeletal system and
463   soft tissues from harmful collision. On both substrates, the cushion pads of ostrich toes not only
464   absorbed collision but also provided additional area to decrease pressure by deforming,
465   especially at high speed. The morphology of toe improved the effect of traction and helped to
466   maintain the balance of COM on sand surface.

467

468

469

Supplemental Information

470

471

472   **Analysis of ostrich running on loose sand.** Raw data for plantar pressure on different parts
473   of ostrich foot (claw, 3rd toe, 4th toe and total). Fig. 10 sand-running was plotted from these dots.

474

475   **Analysis of ostrich running on solid ground.** Raw data for the plantar pressure on
476   different parts of ostrich foot (claw, 3rd toe, 4th toe and total). Fig.10 solid-running was plotted
477   from these dots.

478

479   **Analysis of ostrich walking on loose sand.** Raw data for the plantar pressure on different
480   parts of ostrich foot (claw, 3rd toe, 4th toe and total). Fig.11 sand-walking was plotted from these
481   dots.

482

Analysis of ostrich walking on solid ground. Raw data for the plantar pressure on different parts of ostrich foot (claw, 3rd toe, 4th toe and total). Fig.11 solid-walking was plotted from these dots.

486

Video of ostrich running on loose sand.

488

Video of ostrich running on solid ground.

490

Video of ostrich walking on loose sand.

492

Video of ostrich walking on solid ground.

494

495

Reference

496

1. Dickinson MH, Farley CT, Full RJ, Koehl MAR, Kram R, Lehman S. (2000) How animals move: an integrative view. Science 288: 100-106. doi: 10.1126/science.288.5463.100

2. Li C, Hsieh,T. and Goldman DI. (2012) Multi-functional foot use during running in the zebra-tailed lizard *(Callisaurus draconoides)*. J Exp Biol215: 3293-3308. doi: 10.1242/jeb.061937

3. Li C, Zhang T, Goldman DI. (2013) A terradynamics of legged locomotion on granular media. Science 339: 1408-1412. doi: 10.1126/science.1229163

4. Cavagna GA, Kaneko M. (1977) Mechanical work and efficiency in level walking and running. J Physiol 268: 467-481. doi:10.1113/jphysiol.1977.sp011866

5. Alexander RM. (1991) Energy-saving mechanisms in walking and running. J Exp Biol 160:

507   55-69.

508   6.   Cavagna GA, Willems PA, Legramandi MA, Heglund NC. (2002) Pendular energy
509   transduction within the step in human walking.J Exp Biol 205: 3413-3422.

510   7.   Spence AJ, Revzen S, Seipel J, Mullens C, Full RJ. (2010) Insects running on elastic surfaces.
511   J Exp Biol213: 1907-1920. doi: 10.1242/jeb.042515

512   8.   Geyer H, Seyfarth A, Blickhan, R. (2005) Spring-mass running: simple approximate solution
513   and   application   to   gait   stability.   J   THEOR   BIOL   232:   315-328.   doi:
514   10.1016/j.jtbi.2004.08.015

515   9.   Birn-Jeffery AV, Hubicki CM, Blum Y, Renjewski D, Hurst JW, Daley MA. (2014) Don't
516   break a leg: running birds from quail to ostrich prioritise leg safety and economy on uneven
517   terrain. J Exp Biol 217: 3786-3796. doi: 10.1242/jeb.102640

518   10. Geyer H, Seyfarth A, Blickhan R. (2006) Compliant leg behaviour explains basic dynamics
519   of walking and running. Proc R Soc B 273: 2861-2867. doi: 10.1098/rspb.2006.3637

520   11. Full RJ, Tu MS. (1990) Mechanics of six-legged runners. J Exp Biol 148: 129-146.

521   12. Heglund NC, Fedak MA, Taylor CR, Gavagna GA. (1982) Energetic and mechanics of
522   terrestrial locomotion. IV. Total mechanical energy changes as a function of speed and body
523   size in birds and mammals.J Exp Biol 97: 57-66.

524   13. Collins S, Ruina A, Tedrake R, Wisse M. (2005) Efficient bipedal robots based on passive-
525   dynamic walkers. Science 307: 1082-1085. doi: 10.1126/science.1107799

526   14. Lejeune TM, Willems PA, Heglund NC. (1989) Mechanics and energetics of human
527   locomotion on sand. J Exp Biol 201:2071-2080

528   15. Maladen, R. D., Ding, Y., Li, C., and Goldman, D. I. (2009) Undulatory swimming in sand:
529   subsurface   locomotion   of   the   sandfish   lizard.   Science   325,   314-318.   doi:
530   10.1126/science.1172490

531   16. Marvi H, Gong C, Gravish N, Astley H, Travers M, Hatton RL, Mendelson JR 3rd, Choset H,
532   Hu DL, Goldman DI. (2014) Sidewinding with minimal slip: Snake and robot ascent of
533   sandy slopes. Science 346: 224-229. doi: 10.1126/science.1255718

534   17. Korff WL, McHenry MJ. (2011) Environmental differences in substrate mechanics do not
535   affect sprinting performance in sand lizards (*Uma scoparia and Callisaurus draconoides*). J

536   Exp Biol 214: 122-130. doi: 10.1242/jeb.045682

537 18. Crofts SB, Summers AP. (2011) Biomechanics: swimming in the sahara. Nature 472: 177-
538   178. doi:10.1038/472177a

539 19. Irschick DJ, Jayne BC. (1999) Comparative three-dimensional kinematics of the hindlimb for
540   high-speed bipedal and quadrupedal locomotion of lizards. J Exp Biol 202:1047-1065.

541 20. Li C, Umbanhowar PB, Komsuoglu H, Koditschek DE, Goldman DI. (2009) Sensitive
542   dependence of the motion of a legged robot on granular media. Proc Natl Acad Sci USA106:
543   3029–3034 doi: 10.1073/pnas.0809095106

544 21. Li C, Umbanhowar PB, Komsuoglu H, Goldman DI. (2011) The effect of limb kinematics on
545   the speed of a legged robot on granular media. EXP MECH50: 1383–1393. doi:
546   10.1007/s11340-010-9347-1

547 22. Mazouchova N, Gravish N, Savu A, Goldman DI. (2010) Utilization of granular
548   solidification during terrestrial locomotion of hatchling sea turtles. Biol Lett 6: 398-401. doi:
549   10.1098/rsbl.2009.1041

550 23. Mazouchova N, Umbanhowar PB. Goldman DI. (2013) Flipper-driven terrestrial locomotion
551   of a sea turtle-inspired robot.Bioinspir Biomim 8: 1748-3182. doi: 10.1088/1748-
552   3182/8/2/026007

553 24. Alexander R, Maloiy GMO, Njau R, Jayes AS. (1979) Mechanics of running in the ostrich
554   (*Struthio camelus*). J Zool (Lond) 187: 169-178. doi: 10.1111/j.1469-7998.1979.tb03941.x

555 25. Abourachid A, Renous S. (2000) Bipedal locomotion in ratites (Palaeognatiform): examples
556   of cursorial birds. Ibis 142: 538-549. doi: 10.1111/j.1474-919X.2000.tb04455.x

557 26. Williams JB, Siegfried WR, Milton SJ, Adams NJ, Dean WRJ, Du Plessis MA, Jackson Sue.
558   (1993) Field metabolism, water requirements, and foraging behaviour of wild ostriches in the
559   namib. Ecology 74: 390-404. doi: 10.2307/1939301

560 27. Watson RR, Rubenson J, Coder L, Hoyt DF, Propert MWG, Marsh RL. (2010) Gait-specific
561   energetics contributes to economical walking and running in emus and ostriches. Proc R Soc
562   B278: 2040–2046. doi: 10.1098/rspb.2010.2022

563 28. Rubenson J, Lloyd DG, Heliams DB, Besier TF, Fournier PA. (2011) Adaptations for
564   economical bipedal running: the effect of limb structure on three-dimensional joint

565   mechanics. J R Soc Interface 8: 740-755. doi: 10.1098/rsif.2010.0466

566 29. Smith NC, Wilson A M, Jespers KJ, Payne RC. (2006) Muscle architecture and functional
567   anatomy of the pelvic limb of the ostrich (*Struthio camelus*). J Anat209: 765–779. doi:
568   10.1111/j.1469-7580.2006.00658.x

569 30. Fowler ME. (1991) Comparative clinical anatomy of ratites. J Zoo Wildl Med 22: 204-227.

570 31. El-Gendy SAA, DerbalahA, El-Magd MERA. (2011) Histo-morphological study on the
571   footpad of ostrich (*Struthio camelus*) in relation to locomotion. J Vet Anat 4: 77-97.

572 32. Schaller NU, D'Août K, Villa R, Herkner B, Aerts, P. (2011) Toe function and dynamic
573   pressure distribution in ostrich locomotion. J Exp Biol214: 1123-1130. doi:
574   10.1242/jeb.043596

575 33. Nasuno S, Kudrolli A, Gollub JP. (1997) Friction in granular layers: hysteresis and
576   precursors. PHYS REV LETT79: 949-952.

577 34. Whittle MW. (1999) Generation and attenuation of transient impulsive forces beneath the
578   foot: a review. GAIT POSTURE.10: 264–275. doi:10.1016/S0966-6362(99)00041-70

579 35. Daoud AI, Geissler GJ, Wang F, Saretsky J, Daoud YA, Lieberman DE. (2012) Foot strike
580   and injury rates in endurance runners: a retrospective study. Med Sci Sports Exerc. 44: 1325–
581   1334. doi:10.1249/MSS.0b013e3182465115

582 36. Lieberman DE, Venkadesan M, Werbel WA, Daoud AI, D'Andrea S, Davis IS, Mang'eni
583   RO, Pitsiladis Y.. (2010) Foot strike patterns and collision forces in habitually barefoot
584   versus shod runners. Nature 463: 531-535. doi: 10.1038/nature08723

585 37. Bramble DM., Lieberman DE. (2004) Endurance running and the evolution of *Homo*. Nature
586   432: 345-352. doi:10.1038/nature03052

587 38. Chia K, Schmitt D. (2005) Mechanical energy and effective foot mass during impact loading
588   of walking and running. J Biomech 38: 1387-1395. doi: 10.1016/j.jbiomech.2004.06.020

589 39. Weissengruber GE, Egger GF, Hutchinson JR, Groenewald HB,Elsäser L, Famini D,
590   Forstenpointner G. (2006) The structure of the cushions in the feet of african elephants (
591   *Loxodonta africana*). J Anat 209: 781–792. doi: 10.1111/j.1469-7580.2006.00648.x

592 40. Gefena A, Megido-Ravid M, Itzchak, Y. (2001) In vivo biomechanical behavior of the
593   human heel pad during the stance phase of gait. J BIOMECH 34: 1661–1665. doi:

594   10.1016/S0021-9290(01)00143-9

595 41. Geyer H, Seyfarth A, Blickhan R. (2006) Compliant Leg Behaviour Explains Basic
596   Dynamics of Walking and Running [J]. Proceedings of the Royal Society B Biological
597   Sciences, 273(1603):2861-2867.

598 42. O'Connor S M. (2009). The Relative Roles of Dynamics and Control in Bipedal Locomotion
599   [D]. University of Michigan.

600 43. Hsieh S T, Lauder G V, Wake D B. (2004) Running on Water: Three-Dimensional Force
601   Generation by Basilisk Lizards [J]. Proceedings of the National Academy of Sciences of the
602   United States of America, 101(48):16784.

603 44. Falkingham P L, Gatesy S M. The birth of a dinosaur footprint: subsurface 3D motion
604   reconstruction and discrete element simulation reveal track ontogeny.[J]. Proceedings of the
605   National Academy of Sciences of the United States of America, 2014, 111(51):18279-84.